

Development of Multi-Wavelength-Range High-Resolution Spectrometer for Hydrogen Atomic and Molecular Emission Lines

Keisuke FUJII, Taiichi SHIKAMA, Atsushi IWAMAE¹⁾, Motoshi GOTO²⁾, Shigeru MORITA²⁾ and Masahiro HASUO

Graduate School of Engineering, Kyoto University, Kyoto 606-8501, Japan

¹⁾Japan Atomic Energy Agency, Naka 311-0193, Japan

²⁾National Institute for Fusion Science, Toki 509-5292, Japan

(Received 18 January 2010 / Accepted 22 April 2010)

We have developed a spectrometer specialized for a simultaneous high-resolution measurement of emission spectra of the hydrogen atomic Balmer- α , - β , - γ lines and molecular Fulcher- α ($v' = v'' = 0$) and ($v' = v'' = 2$) ro-vibronic bands, where v' and v'' is the vibrational quantum number. The instrumental widths for the respective wavelength ranges are 0.008, 0.009, 0.010, 0.008, and 0.007 nm. We apply the spectrometer to the observation of emissions from a LHD plasma. The observed profiles of these emission lines and bands show polarization dependence. The absolute intensities of these emissions are also estimated.

© 2010 The Japan Society of Plasma Science and Nuclear Fusion Research

Keywords: LHD, hydrogen, atomic and molecular emissions, Zeeman spectroscopy, peripheral plasma

DOI: 10.1585/pfr.5.S2079

1. Introduction

Dynamics of the neutral hydrogen has a significant influence on the plasma confinement of magnetically confined plasmas [1, 2]. It is demanded to observe behavior of atomic and molecular hydrogen in and around the peripheral regions. Spectroscopic diagnostics is one of the powerful tools. Emission intensities of excited hydrogen atoms and molecules have been analyzed for over a decade. From atomic emission line ratios, the electron density, temperature, and dissociation ratios have been estimated [3–5] from the comparison with a collisional-radiative model of hydrogen developed by Sawada *et al.* [6, 7]. From molecular line ratios, the rotational and vibrational temperatures, which are related to the background gas temperature, have been determined [8, 9]. On the other hand, spatially resolved emission intensities and velocities of hydrogen atoms and molecules have been determined with a technique based on the Zeeman patterns appeared in the emission line shapes by several groups [8, 10, 11].

For simultaneous observation of both the hydrogen intensity ratios and line shapes, it is required to measure several atomic and molecular lines with high resolutions at the same time. Here, we report the development of such a spectrometer.

2. Spectrometer

Figure 1 shows a schematic image of the spectrometer. Light introduced by optical fibers (diameter: 400 μm , NA: 0.15) located just in front of the entrance slit is collimated by a concave mirror (M_c , focal length: 1143 mm),

and then incident on a grating (2400 grooves/mm). The diffracted light beams are focused on different areas of a CCD detector (1024×1024 pixels, $13 \times 13 \mu\text{m}^2/\text{pixel}$, Andor, DV435-BV) by five concave mirrors (M_α , M_β , M_γ , M_{Ful}^0 , M_{Ful}^2 ; focal length: 1143 mm) at the locations which correspond to the wavelengths of the Balmer- α (656 nm), - β (486 nm), - γ (434 nm) lines and the Q branch of the Fulcher- α ($v' = v'' = 0$: 602–604 nm), ($v' = v'' = 2$: 622–625 nm) ro-vibronic transition bands. Here, v' and v'' are the vibrational quantum numbers of the upper and lower states, respectively. The incident angle to the grating is set to be 39.5 degrees for enough separations of the five focusing mirrors. The diffraction angles β for the five wavelengths are shown in Table 1.

The off-axis reflections at the concave mirrors cause comatic aberration and astigmatism. We set the reflection angle to be 4.1 degrees which is the smallest angle de-

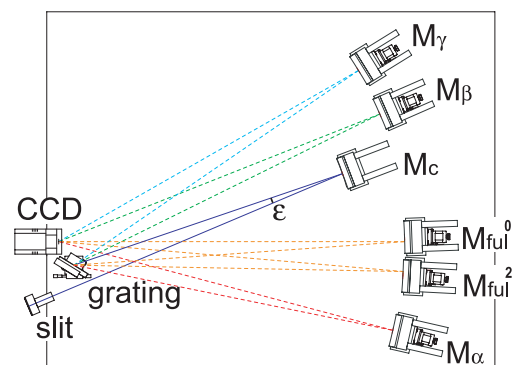


Fig. 1 A schematic image of the spectrometer.

author's e-mail: fujii.keisuke@fs4.ecs.kyoto-u.ac.jp

Table 1 The diffraction angles and reflection angles of the focusing mirrors, and the measured instrumental width (FWHM) for five hydrogen emission lines.

	Balmer- α	Balmer- β	Balmer- γ	Fulcher- α $\nu'=\nu''=0$	Fulcher- α $\nu'=\nu''=0$
diffraction angle [degree]	69.9	32.0	23.9	54.3	59.4
reflection angle [degree]	3.3	4.6	4.7	4.1	3.9
instrumental width [nm]	0.008	0.009	0.010	0.008	0.007

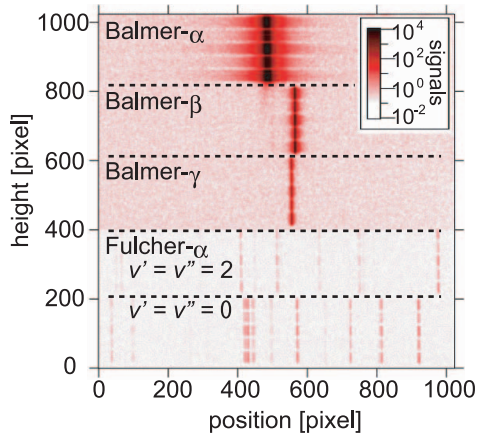


Fig. 2 A two dimensional image for the emission from a hydrogen low-pressure discharge tube focused on the CCD detector. The entrance slit width is $20\ \mu\text{m}$. The areas for the observed emissions are distinguished with the dashed lines. Since the molecular emissions are weak, the CCD exposure time is 10 times longer than that for the atomic lines.

terminated by the size of the optical components we used. Even in this condition, the mismatch between the reflection angles of the collimating mirror and that of the focusing mirror makes the focused image of the fiber exit on the CCD detector to be distorted. Using a ray-tracing and multidimensional-minimization calculation, we optimized the configuration of the optical components of the spectrometer. In this calculation, we traced 500,000 rays left from the five fiber exits aligned with a center distance of $500\ \mu\text{m}$, assuming the pure geometrical optics. The width of the entrance slit is set to be $20\ \mu\text{m}$ and the rays are assumed to leave uniformly from the fiber exits. We calculated the image focused on the CCD detector after reflections by the mirrors and diffraction by the grating. The parameters to be optimized are the positions of the five focusing mirrors and the CCD detector. We minimized the instrumental widths of the five focused images. The optimized reflection angles of the five focusing mirrors are shown in Table 1.

Figure 2 shows an example of the focused images obtained for the emission from a hydrogen low-pressure discharge tube. The horizontal axis is parallel to the direction of the wavelength dispersion while the vertical axis is parallel to the slit. The boundaries of the areas on the CCD detector for respective emissions are shown by the dashed lines. The five spots aligned vertically in each area correspond to the five fiber exits at the entrance slit. The verti-

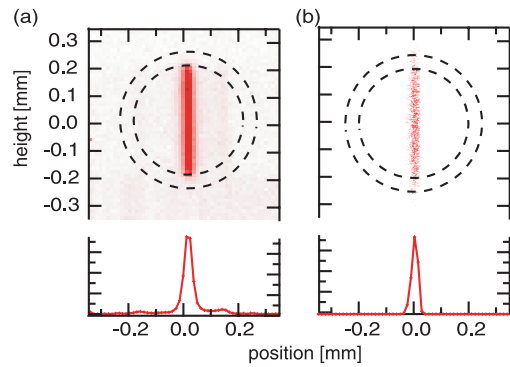


Fig. 3 (a) The two dimensional focused image measured for the thorium emission of $602.1\ \text{nm}$ and (b) that calculated by the ray-tracing code at the entrance slit width of $20\ \mu\text{m}$. The horizontal axis is parallel to the direction of the wavelength dispersion. The dotted circles show the image of the optical fiber exit at the entrance slit. The horizontal cross sections of the focused images are shown in the bottom sides. It is noted there are some weak thorium emission lines in the line wing in (a).

cal instrumental width is $400\ \mu\text{m}$. The astigmatism is small enough to avoid overlapping the fiber images.

The instrumental resolution for the five wavelength ranges are estimated from the line widths of thorium emission lines of a thorium-argon hollow cathode discharge lamp (Heraeus, P858A), the line widths of which are narrow enough. Figure 3 (a) shows the observed focused image of the thorium emission at $602.1\ \text{nm}$. The horizontal width (FWHM) of this line is obtained to be $36\ \mu\text{m}$ ($0.008\ \text{nm}$ in wavelength). The instrumental function for Fulcher- α band $\nu' = \nu'' = 0$ Q1 emission ($601.8\ \text{nm}$) calculated by the ray-tracing code is shown in Figure 3 (b). The calculated width is $28\ \mu\text{m}$ ($0.005\ \text{nm}$ in wavelength). In this calculation, we neglect the effect of the diffraction limit of the grating, of which FWHM is $0.002\ \text{nm}$ for the light of $600\ \text{nm}$. It may be a dominant reason for the difference between the measurement and calculation. The instrumental widths for the five wavelength ranges are shown in Table 1.

We converted the horizontal pixels of an image like Fig. 2 to the light wavelength with the thorium-argon discharge lamp because there are many lines in the visible range. We obtained emission spectra by binning the intensities over the vertical pixels in each fiber image. The absolute sensitivities of the spectrometer are calibrated with a standard lamp and a standard reflection sphere (Labsphere, USS-600C).

3. Application to LHD Plasmas

We applied the spectrometer to the observation of LHD periphery plasmas. The poloidal cross section of LHD and the line of sight we used are shown in Fig. 4. We measured polarization resolved spectra with a polarization separation optics (PSO) [3] because the spectral shapes are affected by the strong magnetic fields of LHD depending on their polarization. The direction of the extraordinary polarization of the PSO was set to be the magnetic direction at the inner ergotic layer.

The spectra were measured with 370 ms exposure time of the CCD detector, during a hydrogen discharge heated

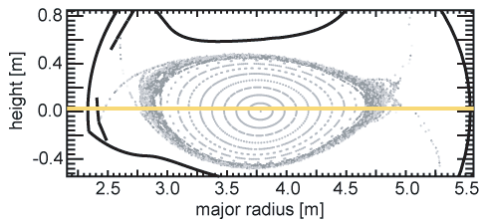


Fig. 4 Poloidal cross section of the LHD and the measurement line of sight.

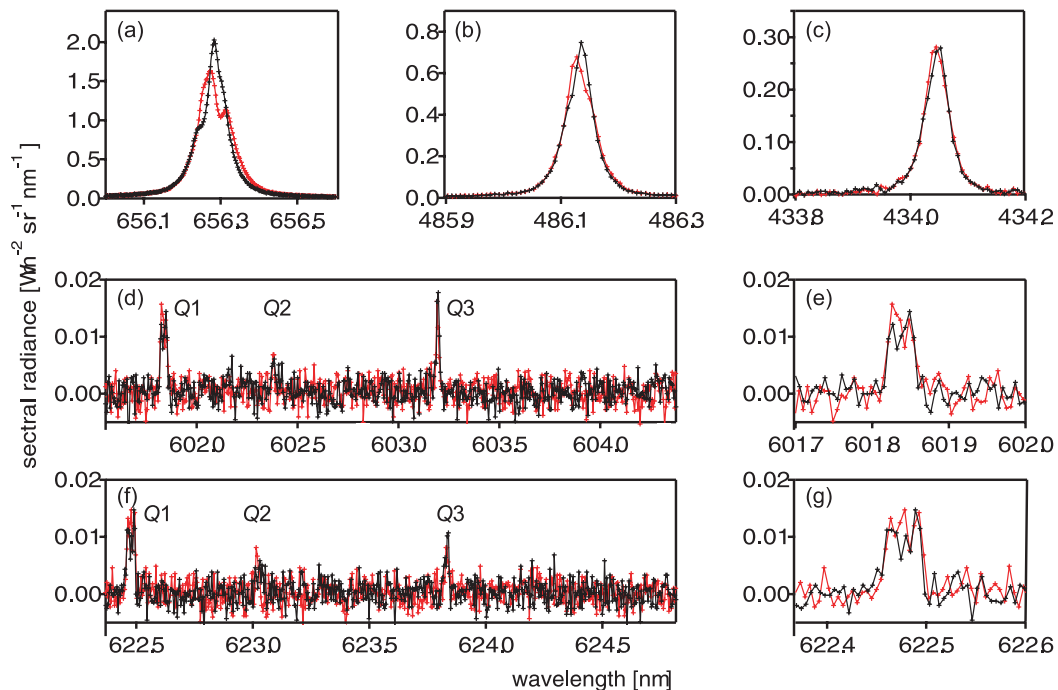


Fig. 5 The observed spectra of the emissions from the LHD periphery plasma. (a), (b), (c), (d), and (f) show the hydrogen Balmer- α , - β , - γ lines and Fulcher- α $v' = v'' = 0$ and $v' = v'' = 2$ transition bands, respectively. The spectra of ordinary polarization are shown by the red lines and the black lines show those of extraordinary polarization. The expanded spectra for the $Q1$ emission lines of hydrogen molecules are shown in (e) and (g).

by the electron cyclotron heating (ECH) at the input power of 3.7 MW. The line-averaged electron density and the electron temperature at the plasma axis were $1 \times 10^{19} \text{ m}^{-3}$ and 4 keV, respectively. An example of the observed spectra is shown in Fig. 5. The polarization dependences are clearly observed in the Balmer- α and Fulcher- α $Q1$ spectra. Those of the Balmer- β and - γ line shapes were also detected. They were relatively small since the Zeeman split of the spectrum is proportional to the square of its wavelength [8], while the Doppler broadening is proportional to the wavelength. We analyzed the observed atomic spectra with a fitting calculation described in Ref. [10], and we confirmed the degrees of the Zeeman splittings of the observed spectra are consistent with the vacuum magnetic field in the edge regions. The absolute intensities of these emissions are estimated from the areas of the measured spectra, and the result of which are shown in Table 2.

4. Acknowledgment

This work was supported by the National Institute for Fusion Science (NIFS08KOAP020) and in part by Grant-in-Aid for Scientific Research (B) (No. 21340170).

Table 2 The intensities of the observed hydrogen emission lines.

Intensity [$\text{W m}^{-2} \text{ sr}^{-1}$]	Balmer- α	Balmer- β	Balmer- γ	Fulcher- α	
				$v' = v'' = 0$	$v' = v'' = 2$
	3.6×10^{-1}	1.0×10^{-1}	3.5×10^{-2}	4.7×10^{-4}	4.8×10^{-4}
				1.2×10^{-4}	1.1×10^{-4}
				1.8×10^{-4}	2.8×10^{-4}

- [1] F. Wagner *et al.*, Phys. Rev. Lett. **49**, 1408 (1982).
- [2] N. Ohyaabu *et al.*, Phys. Rev. Lett. **84**, 103 (2000).
- [3] H. Kubo, H. Takenaga, K. Sawada, T. Nakano, S. Kobayashi, S. Higashijima, N. Asakura and K. Shimizu, J. Nucl. Mater. **337**, 161 (2005).
- [4] A. Pospieszczyk, Ph. Mertens, G. Sergienko, A. Huber, V. Philipps, D. Reiter, D. Rusbult, B. Schweer, E. Vietzke and P. T. Greenland, J. Nucl. Mater. **266**, 138 (1999).
- [5] A. Escarguel, B. Pegourie1, J. Hogan, C. De Michelis, Y. Corre, A. Azeroual, J. M. Ane, R. Guirlet, J. Gunn, H. Capes, L. Godbert-Mouret, M. Koubiti and R. Stamm, Plasma Phys. Control. Fusion **43**, 1733 (2001).
- [6] K. Sawada, K. Eriguchi and T. Fujimoto, J. Appl. Phys. **73**, 8122 (1993).
- [7] K. Sawada and T. Fujimoto, J. Appl. Phys. **73**, 8122 (1993).
- [8] T. Shikama, S. Kado, H. Zushi and S. Tanaka, Phys. Plasmas **14**, 072509 (2007).
- [9] U. Fantz and B. Heger, Plasma Phys. Control. Fusion **40**, 2023 (1998).
- [10] A. Iwamae, M. Hayakawa, M. Atake, T. Fujimoto, M. Goto and S. Morita, Phys. Plasmas **12**, 042501 (2005).
- [11] T. Shikama, S. Kado, H. Zushi, M. Sakamoto, A. Iwamae and S. Tanaka, Plasma Phys. Control. Fusion **48**, 1125 (2006).